



Article

Appraisal of Daily Temperature and Rainfall Events in the Context of Global Warming in South Australia

Federico Ferrelli ^{1,*}, Melisa Pontrelli Albisetti ², Andrea Soledad Brendel ¹, Andrés Iván Casoni ³ and Patrick Alan Hesp ²

- Instituto Argentino de Oceanografía (IADO), Universidad Nacional del Sur (UNS)-CONICET, Florida 8000 (Camino La Carrindanga km 7,5) Complejo CCT CONICET B8000FWB, Bahía Blanca 8000, Argentina; asbrendel@iado-conicet.gob.ar
- Beach and Dune Systems (BEADS) Laboratory, College of Science and Engineering, Flinders University, Bedford Park 5042, Australia; melisa.albisetti@flinder.edu.au (M.P.A.); patick.hesp@flinders.edu.au (P.A.H.)
- Planta Piloto de Ingeniería Química (PLAPIQUI), Universidad Nacional del Sur (UNS)-CONICET, Florida 8000 (Camino La Carrindanga km 7,5) Complejo CCT CONICET B8000FWB, Bahía Blanca 8000, Argentina; acasoni@plapiqui.edu.ar
- * Correspondence: fferrelli@criba.edu.ar

Abstract: In recent decades, there have been significant problems worldwide related to global warming and the intensification of extreme temperature and rainfall events. This research evaluated daily temperature and rainfall indices trends to identify whether warming signals have occurred in South Australia over the past fifty years. Extreme cold, hot, and rainfall events were calculated using climatic data from 37 weather stations. A Mann–Kendall test was used for trend analysis with Sen's estimator. As a result, we determined that for the 1970–2021 period, the maximum and minimum temperatures increased by 1.1 and 0.7 °C, respectively, while precipitation had a negative trend (–52.2 mm per period). Since statistical significance was found in analysing extreme cold and hot events, we find that warming signals have several impacts on South Australia. In the case of rainfall events, we identified a heterogeneous pattern characterised by a reduction in the annual amount and an increase in extreme rainfall events. The findings enable us to conclude that the area shows signs of global warming that could affect the intensity and magnitude of droughts. This information is essential for continuing with current management strategies to adapt and mitigate the effects of global warming in South Australia.

Keywords: rainfall and temperature trends; climate change; South Australia; Southern Hemisphere



Citation: Ferrelli, F.; Pontrelli Albisetti, M.; Brendel, A.S.; Casoni, A.I.; Hesp, P.A. Appraisal of Daily Temperature and Rainfall Events in the Context of Global Warming in South Australia. *Water* **2024**, *16*, 351. https://doi.org/10.3390/w16020351

Academic Editor: Renato Morbidelli

Received: 4 December 2023 Revised: 3 January 2024 Accepted: 15 January 2024 Published: 21 January 2024



Copyright: © 2024 by the authors. Licensee MDPI, Basel, Switzerland. This article is an open access article distributed under the terms and conditions of the Creative Commons Attribution (CC BY) license (https://creativecommons.org/licenses/by/4.0/).

1. Introduction

Global warming is a critical issue, causing significant changes to the Earth's climate and natural systems, with far-reaching consequences for human society and the environment [1]. The increase in global temperatures is mainly due to human activities such as burning fossil fuels and deforestation, resulting in rising sea levels, more frequent and intense heatwaves, droughts, floods, severe storms, and changes in precipitation patterns [2,3]. Furthermore, global warming affects ecosystems, biodiversity, agriculture and food security, water resources, and human health and well-being [4,5]. It also contributes to economic and social inequalities as vulnerable populations and developing countries are often the hardest hit by the effects of climate change [6].

Addressing global warming requires urgent action to reduce greenhouse gas emissions and transition to a low-carbon economy [7]. Therefore, it will require a coordinated international effort involving governments, businesses, and individuals to change energy production and use, transportation, land use, and waste management [8].

Australia is one of the major countries in the Southern Hemisphere and has been heavily affected by global warming. The continent has experienced record-breaking temperatures, drought, and strong winds, with the summer of 2019–2020 being the hottest on

Water 2024, 16, 351 2 of 18

record [9]. The devastating bushfire season of 2019–2020 destroyed millions of hectares of land, killed wildlife and livestock, and claimed several human lives [10–12]. Global warming also affects Australia's marine ecosystems, with rising sea temperatures and ocean acidification causing coral bleaching and other negative impacts on marine life [13].

The study area for this research is South Australia (SA), a state located in the southern central part of the country. It shares its borders with Western Australia to the west, the Northern Territory to the north, Queensland to the northeast, New South Wales to the east, and Victoria to the southeast. The state covers an area of 983,400 km² and has a population of around 1.8 million people [14]. Rainfall decreases from south to north and also east to west, with the highest precipitation in the southeast and lower values in the northeast and west. The temperature is highest in the north and decreases towards the south (Figure 1). South Australia showcases diverse rainfall patterns, with coastal areas exhibiting a Mediterranean climate characterised by mild, wet winters and warm to hot, dry summers [15]. Conversely, inland regions often endure arid or semi-arid conditions marked by sporadic, lower rainfall, leading to less distinct wet and dry seasons. The region's climate is notably shaped by its proximity to ocean currents. The Great Australian Bight, positioned south of SA, experiences the influence of the cold Southern Ocean waters. Consequently, this exerts a moderating effect on coastal temperatures. Moreover, temperature fluctuations vary significantly across SA. Coastal areas benefit from milder temperatures owing to the ocean's influence, while inland regions encounter more pronounced temperature swings, experiencing hotter summers and colder winters. These climatic variations contribute to a diverse landscape in SA, encompassing coastal plains, arid deserts, fertile agricultural zones, and unique ecosystems such as the Flinders Ranges and the Outback [15,16].

SA is renowned for its diverse landscapes, ranging from the arid Outback to the fertile wine regions of the Barossa Valley and Adelaide Hills. The area produces high-quality food, wine, and mineral resources such as copper, gold, and uranium. The state's largest city, Adelaide, serves as its capital and is home to over 75% of its population. SA is a crucial economic hub, with agriculture, mining, manufacturing, and tourism all contributing significantly to its economy. However, the region has experienced significant changes in climate patterns due to climate change and global warming [17]. Partly in response to climate and partly due to government-led adaptation measures, SA has become a leader in renewable energy, with significant investments in wind and solar power [18,19].

Extreme temperature events require strict risk management and adaptation strategies that rely on accurately understanding climate patterns [20]. Assessing daily temperature and rainfall events is crucial in understanding the impact of global warming at a regional or local scale. Daily analysis is vital because it provides a highly accurate way to identify the intensity and magnitude of thermal and rainfall variability [21]. Despite the critical significance of analysing climate variability with daily measurements, studies on extreme daily temperature and rainfall events in South Australia have been scarce. We have limited knowledge about how climatic trends in extreme temperature and precipitation events affect this region. For all these reasons, this study aimed to identify warming signals and changes in rainfall patterns over the past 50 years in SA to improve the management of climate risk, adaptation, and mitigation practices required in the area.

Water 2024, 16, 351 3 of 18

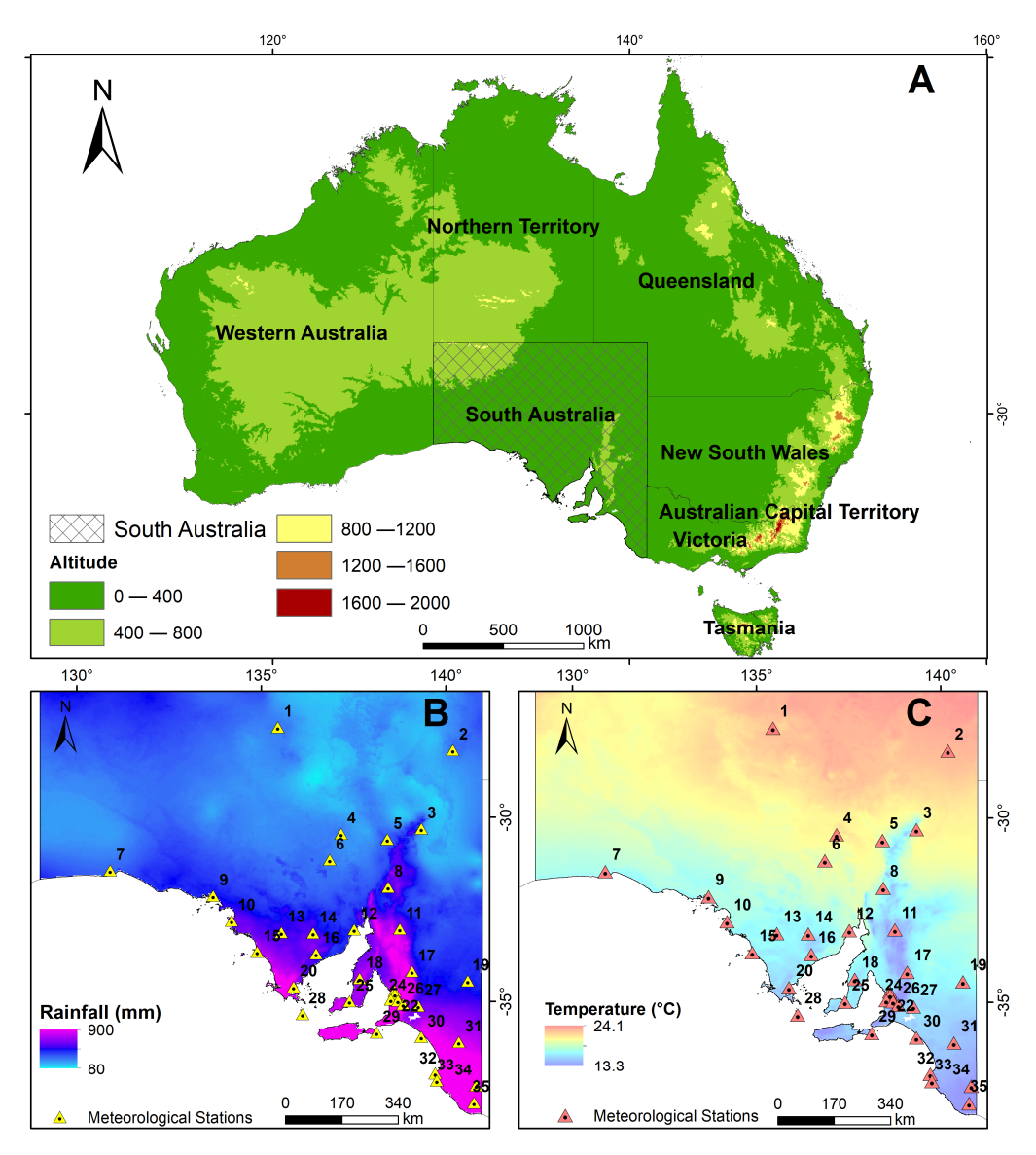


Figure 1. (A) Location map, (B) Rainfall spatial distribution with the weather stations, (C) thermal spatial distribution with the weather stations.

2. Materials and Methods

Maximum and minimum temperatures, standard deviation, and annual precipitation were calculated from 37 weather stations in SA (Table 1). The meteorological information was obtained for different periods but standardised between 1970 and 2021. The data were downloaded from the Bureau of Meteorology of the Australian Government (http://www.bom.gov.au/ (accessed on 30 December 2023).

The time series were pre-processed using automated scripts to correct mistakes such as topographical errors, inconsistencies in the data, and labelling issues following the method described in [22]. The time series underwent pre-processing that involved structuring data into tables with columns containing daily maximum and minimum temperatures ($^{\circ}$ C) and precipitation (mm per day). Additionally, the designated mask value representing "NoData" was recognised as -99.9. Throughout the reformatting and conversion stages, automatic scripts were utilised to rectify topographical errors, inconsistencies in the NoData mask, and mislabelling, as outlined in [22].

Water **2024**, 16, 351 4 of 18

Table 1. Weather stations, location, height, period, mean maximum and minimum temperature, and precipitation annual amounts with their standard deviation.

ID	Weather Station	Lat	Long	Altitude (m)	Period	Tmax (°C)	Tmin (°C)	Pp (mm)
1	Woomera Aerodrome	-31.16	136.86	167	1949–2021	25.8 ± 6.5	12.7 ± 5.1	179.8 ± 81.4
2	2 Andamooka		137.17	76	1965–2021	26.1 ± 6.6	13.8 ± 5.7	181.9 ± 100.9
3	Oodnadatta Airport	-27.56	135.45	117	1939–2021	29.1 ± 6.7	12.7 ± 5.3	168.8 ± 99.7
4	Arkaroola	-30.31	139.34	318	1938–2021	25.7 ± 6.4	11.5 ± 6.1	246.8 ± 160.9
5	Leigh Creek Airport	-30.6	138.42	259	1982–2021	26.3 ± 6.9	12.8 ± 5.9	207.8 ± 102.2
6	Moomba Airport	-28.18	140.2	38	1995–2021	29.6 ± 6.8	15.5 ± 6.7	161.7 ± 126.3
7	Ceduna Amo	-32.13	133.7	15	1939–2021	23.5 ± 4.05	10.4 ± 3.5	293.4 ± 84.4
8	Cleve	-33.7	136.49	193	1986–2021	22.5 ± 4.7	11.6 ± 3.3	399.1 ± 97.2
9	Kimba	-33.14	136.41	280	1920-2021	23.8 ± 5.9	10.4 ± 4.1	341.9 ± 106.1
10	Kyancutta	-33.13	135.55	59	1930-2021	25.2 ± 5.8	9.3 ± 3.6	310.6 ± 79.09
11	Elliston	-33.65	134.89	7	1882–2021	21.5 ± 3.5	11.8 ± 2.9	422.6 ± 100.1
12	Streaky Bay	-32.81	134.2	45	1865–2021	23.3 ± 4.61	13.2 ± 2.9	371.8 ± 97.6
13	Nullarbor	-31.45	130.9	64	1888–2021	23.8 ± 3.5	10.8 ± 3.94	186.9 ± 147.8
14	Neptune Island	-35.34	136.12	32	1957–2021	18.6 ± 2.58	13.8 ± 1.9	403.2 ± 143.9
15	Whyalla Aero	-33.05	137.52	9	1945–2021	23.7 ± 4.8	11.5 ± 4.7	243.7 ± 96.1
16	North Shields (Port Lincoln Aws)	-34.6	135.88	9	1992–2021	22.2 ± 3.7	11.3 ± 3.3	379.6 ± 92.8
17	Hawker	-31.9	138.44	340	1882–2021	24.5 ± 6.7	10.8 ± 5.4	300.4 ± 121.1
18	Adelaide Airport	-34.95	138.52	2	1955–2021	21.5 ± 4.7	11.5 ± 3.4	438.4 ± 102.8
19	Adelaide West Terrace	-34.93	138.58	29	1839–2021	21.8 ± 5.05	12.02 ± 3.38	521.3 ± 115.7
20	Cape Jaffa	-36.97	139.72	17	1991–2021	19.2 ± 3.9	12.4 ± 2.3	488 ± 111.8
21	Cape Willoughby	-35.84	138.13	55	1881–2021	18.1 ± 2.8	12.8 ± 2.4	528.6 ± 129.8
22	Coonawarra	-37.29	140.83	57	1985–2021	20.4 ± 5.06	8.1 ± 2.4	563.3 ± 112.6
23	Edinburgh RAAF	-34.71	138.62	17	1972–2021	22.6 ± 5.46	11.1 ± 3.9	417.2 ± 112.9
24	Eudunda	-34.18	139.09	420	1882-2021	21.1 ± 6.03	9.2 ± 3.4	$445.1 \!\pm 120.7$
25	Keith	-36.1	140.36	29	1906–2021	22.3 ± 5.58	9.2 ± 2.9	453.9 ± 101.8
26	Loxton Research Centre	-34.44	140.6	30	1984–2021	23.9 ± 5.9	9.08 ± 4.01	260 ± 77.6
27	Maitland	-34.37	137.67	185	1879–2021	21.7 ± 5.4	11.24 ± 4.02	487.8 ± 131.4
28	Maningie	-35.96	139.34	3	1864-2021	21.03 ± 4.1	10.41 ± 2.7	441.4 ± 145.1
29	Mount Barker	-35.07	138.85	359	1861–2021	20.2 ± 5.2	8.2 ± 2.7	748.5 ± 193.2
30	Mount Gambier Aero	-37.75	140.77	63	1941–2021	19.02 ± 4.4	8.2 ± 2.3	714.6 ± 123.5
31	Mount Lofty	-34.98	138.71	685	1985–2021	22.9 ± 5.1	8.7 ± 2.8	791.4 ± 123.6

Water **2024**, 16, 351 5 of 18

Table 1. Cont.

ID	Weather Station	Lat	Long	Altitude (m)	Period	Tmax (°C)	Tmin (°C)	Pp (mm)
32	Murray Bridge	-35.12	139.26	33	1885-2021	15.9 ± 4.8	9.8 ± 3.5	714.6 ± 205.2
33	Parafield Airport	-34.8	138.63	10	1929–2021	22.5 ± 5.4	10.8 ± 3.8	431.2 ± 103.6
34	Price	-34.3	138	2	1944–2021	22.8 ± 4.6	11.2 ± 3.7	322.8 ± 88.9
35	Robe	-37.16	139.76	3	1860-2021	18.1 ± 3.3	10.9 ± 2.01	621.5 ± 134.8
36	Warooka	-34.99	137.4	53	1861–2021	21.2 ± 4.5	11.6 ± 3.07	438.7 ± 97.8
37	Yongala	-33.03	138.76	521	1881–2021	22.01 ± 6.6	7.4 ± 4.3	345.4 ± 125

Then, we conducted quality control and homogeneity assessments using the RClimDex Software [23] and RHTest V4 Software, both of which were created by the Expert Team on Climate Change Detection and Indices (ETCCDI) and are freely available. RHTest V4 uses a penalised maximal *t*-test and a maximal F-test set in a recursive algorithm, which allows for temporal homogeneity analysis of daily data from the 37 weather sites [24–26]. The objective of climatic homogenisation was to rectify observations by accounting for the fact that alterations in the corrected data were solely due to climate-related variations. Factors not related to climate included shifts in station placement, environmental changes, and alterations in instrumentation, all of which could potentially influence the authentic trends in the data [26]. Due to these factors, we were able to obtain missing data and outliers. It is worth noting that some stations had periods with missing information. Therefore, we extended the study period to 1970–2021 to establish statistical significance in this research.

We have employed gap-filling techniques to complete the time series of the 37 weather stations. To achieve this, we utilised Principal Component Analysis (PCA), an effectively used method to fill gaps in climate time series [21,22,27,28]. This approach enables the creation of a new set of variables by linearly combining the original variables, thereby effectively capturing most of the observed variance in the original data. We computed initial guess values from linear models between each station and its neighbours.

Subsequently, we computed daily extreme temperature and rainfall events defined by the ETCCDI, including hot and cold extreme events and other indices described in Table 2. These provide a comprehensive overview of temperature and rainfall statistics. Zhang et al. [29] reviewed these indices, which are composed of percentile-based absolutes, duration, and threshold indices [30,31]. In that regard, we added maximum temperature (Tmax) and minimum temperature (Tmin). As such, we applied 23 indices subdivided into four categories: user-defined indices, extreme hot temperature events, Extreme cold temperature events, and rainfall events (Table 2). We assessed these indices at two spatial scales. The first corresponds to the local analysis, considering the 37 weather stations. The second is related to the mean values of the meteorological information available (37 weather stations). Ferrelli et al. [21] employed the same method to examine the effects of global warming on the Pampas (Argentina).

Finally, we calculated linear trends (at the local and regional scale) in extreme temperature and rainfall indices using the non-parametric Mann–Kendall test [32,33] with a significance threshold of α = 0.05. Moreover, to quantify rates of change, we applied Sen's slope estimator (Sen 1968) using the "trend" package [34]. The use of this technique has two benefits. Firstly, it is a non-parametric test, so the data do not need to be normally distributed. Secondly, the inhomogeneous time series used in this test resulted in poor sensitivity to abrupt breaks. The data values are assessed as an organised time series [35]. Some research shows that persistence, serial correlation, and scaling hypotheses can increase the probability of rejecting the correct null hypothesis [36]. However, we initially processed the dataset to remove the serial correlation's influence on the test's results.

Water 2024, 16, 351 6 of 18

Table 2. Daily temperature and precipitation indices. Modified from [21,26,31]. We presented hot extremes, cold extremes, precipitation extremes, and user-defined indices separately.

Index ID	Index Name	Definition	Units					
	Te	emperature indices-User defined						
Tmax	Maximum temperature	The annual mean value of daily maximum temperature for the period 1970–2021	°C					
Tmin	Minimum temperature	The annual mean value of daily minimum temperature for the period 1970–2021	°C					
Extreme hot temperature events								
TXx	Max Tmax	The maximum monthly value of the daily maximum temp	°C					
TNx	Max Tmin	The maximum monthly value of the daily minimum temp	°C					
TX90p	Warm days	Percentage of days when TX > 90th percentile	Days					
DTR	Diurnal temperature range	The monthly mean difference between TX and TN	°C					
SU25	Summer days	Annual count when TX (daily maximum) > 25 °C	Days					
TR20	Tropical nights	Annual count when TN (daily minimum) > 20 $^{\circ}$ C	Days					
TN90p	Warm nights	Percentage of days when TN > 90th percentile	Days					
	E	xtreme cold temperature events						
TXn	Min Tmax	The monthly minimum value of the daily maximum temp	°C					
TNn	Min Tmin	The monthly minimum value of the daily minimum temp	°C					
FD0	Frost days	Annual count when TN (daily minimum) < 0 $^{\circ}$ C	Days					
		Rainfall events						
PRCPtot	Annual total wet-day precipitation	Annual total PRCP in wet days (RR > 1 mm)	mm					
CDD	Consecutive dry days	Maximum number of successive days with RR < 1 mm	Days					
CWD	Consecutive wet days	Maximum number of consecutive days with RR > 1 mm	Days					
SDII	Simple daily intensity index	Annual total precipitation divided by the number of wet days (defined as PRCP \geq 1 mm) in the year	mm/day					
RX1day	Max 1-day precipitation amount	Monthly maximum 1-day precipitation	mm					
Rx5day	Max 5-day precipitation amount	Monthly maximum consecutive 5-day precipitation	mm					
R10	Number of heavy precipitation days	Annual count of days when PRCP > 10 mm	Days					
R20	Number of very heavy precipitation days	Annual count of days when PRCP > 20 mm	Days					
R30	Number of extreme precipitation days	Annual count of days when PRCP > 30 mm	Days					
R95p	Very wet days	Annual total PRCP when RR > 95th percentile	mm					
R99p	Extremely wet days	Annual total PRCP when RR > 99th percentile	mm					

3. Results

3.1. Temperature and Rainfall Trends

The maximum temperature has increased throughout the entire weather station suite analysed in SA, with most of the area experiencing significant changes (100% of the weather stations), showing a generally increasing trend. The minimum temperature in the majority of SA (86% of weather stations) has demonstrated a positive trend, with the exception of Cape Jaffa, which displayed a negative tendency. However, it is important to note that

Water **2024**, 16, 351 7 of 18

this change exhibited a non-significant trend, with the slope indicating negligible climatic change over time (-0.2 °C/period, p = 0.88). The annual precipitation during wet days has decreased (78% of weather stations), but positive trends have been identified in the coastal zones (+22 mm/period, p = 0.83) and in the north of the study area (Figure 2).

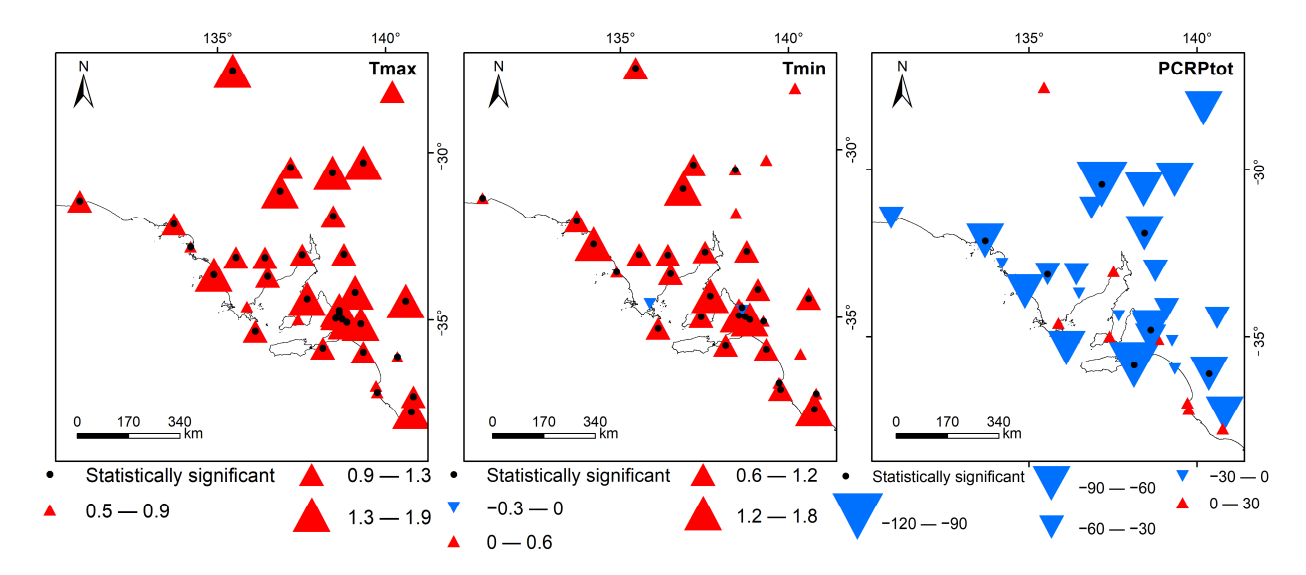


Figure 2. Trends and significance of maximum temperature (Tmax), minimum temperature (Tmin), and annual precipitation during wet days (PCRPtot). The triangles indicate positive trends (in red) and negative trends (in blue), along with their intensity. The black dots indicate the statistical significance of the slope.

Figure 3 presents the regional behaviour of maximum (Tmax) and minimum Temperature (Tmin) and the annual total wet-days precipitation (PCRPtot) for the 1970–2021 period. We identify a significant increase in the Tmax (+1.1 $^{\circ}$ C, p < 0.01), as well as in Tmin (+0.7 $^{\circ}$ C, p < 0.01). In the case of PCRPtot, the trend presented a non-significative decrease (–52.2 mm/period, p = 0.73) (Figure 3).

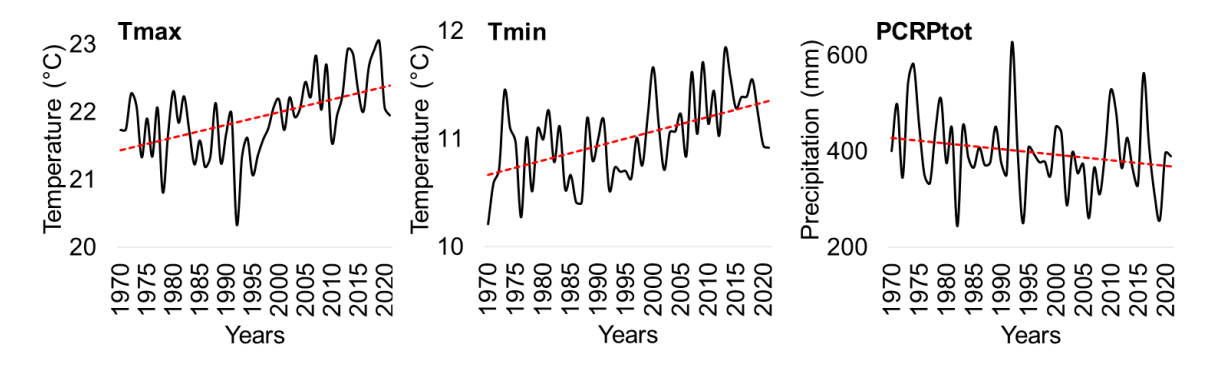


Figure 3. Regional behaviour of maximum temperature (Tmax), minimum temperature (Tmin), and the annual total wet-days precipitation (PCRPtot) for the period 1970–2021. The red dot-dash line indicates the slope for the study period.

3.2. Extreme Hot Temperature Events

Extreme hot events in SA have shown a general increase from 1970 to 2021. These indices are the most relevant indicators of global warming in the region. In this context, most indices showed positive and significant trends across the entire area. Hotter Days (TXx) have demonstrated an increase ranging from $3.7\,^{\circ}\text{C}$ to $2.4\,^{\circ}\text{C}$. Positive trends were statistically significant (p < 0.05), while negative ones were not (p > 0.05). The maximum monthly value of the daily minimum temp (TNx) showed a similar pattern, with 98% of the region showing positive trends (Figure 4).

Water **2024**, 16, 351 8 of 18

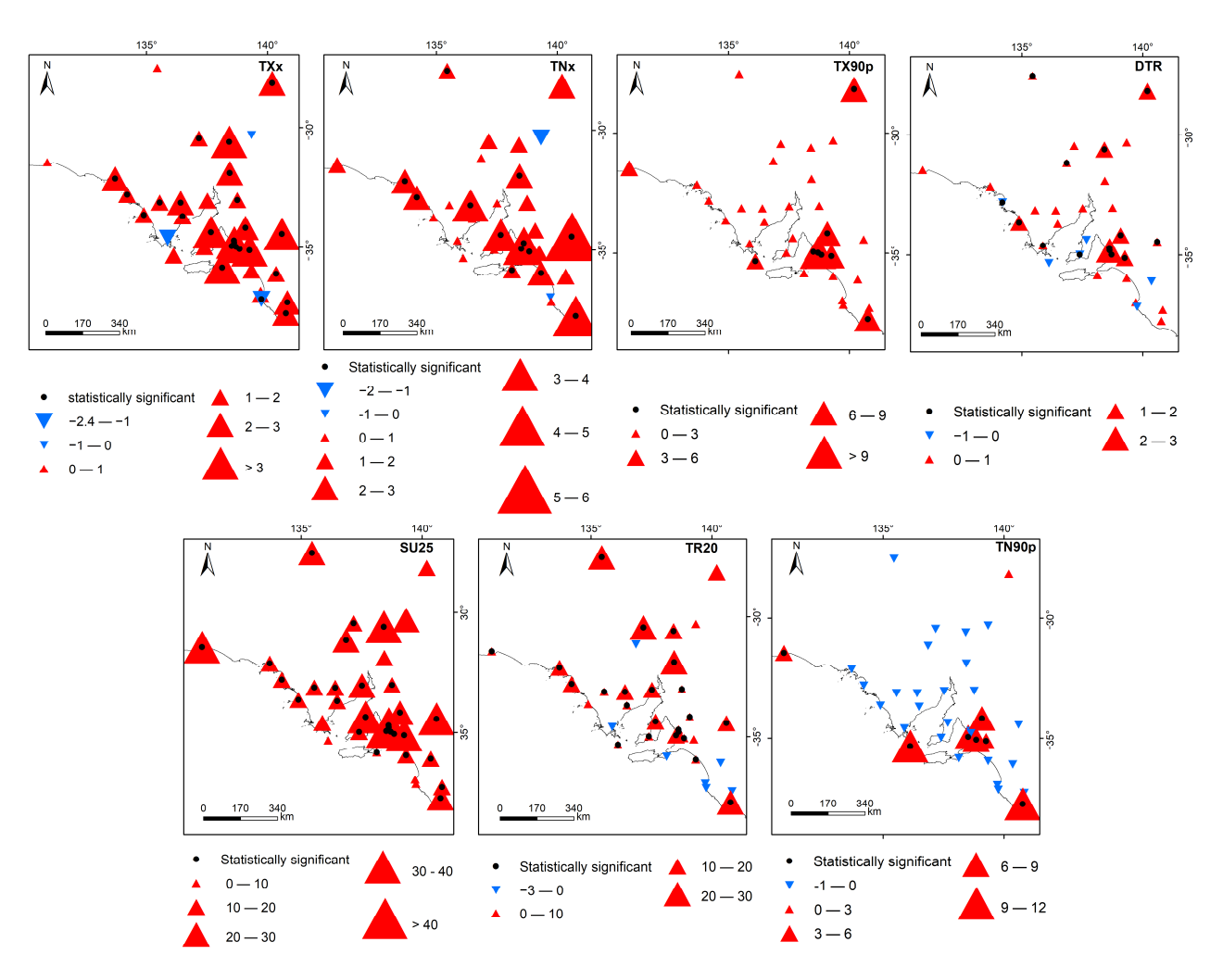


Figure 4. Trends and significance of the extreme hot events. Results for hottest days (TXx), the maximum monthly value of the daily minimum temp (TNx), warm nights (TX90p), DTR, summer days (SU25), tropical nights (TR20), and warm days (TN90p) are shown. The triangles indicate positive trends (in red) and negative trends (in blue), along with their intensity. The black dots indicate the statistical significance of the slope.

The most significant change was observed in Summer Days (SU25), with 100% of weather stations showing positive trends and over 81% being statistically significant. We analysed the same pattern with Warm Days (TX90p), where all weather stations showed a positive tendency, but statistical significance was only identified in 18.9% of the area. Moreover, Tropical Nights (TR20) increased significantly in most of SA, except for the coastal region, where this index showed negative values. Warm Nights (TN90p), on the other hand, showed a general negative trend (Figure 4).

At a regional scale, Hottest Days (TXx), Summer Days (SU25), and Tropical Nights (TR20) showed the highest increase (p < 0.01) with a total of 1.9 °C, 20.7 days, and 7.8 days per period, respectively. The sharp rise in SU25 and TR20 occurred from 2000 to 2021 at rates of 0.68 and 0.21 days per year, respectively. Warm Days (TN90p) and Nights (TX90p) registered a moderate increase (p < 0.05) with regional values of 5.8 and 0.8 days per period, respectively. The other hot extremes lacked regional significance (Figure 5).

Water **2024**, 16, 351 9 of 18

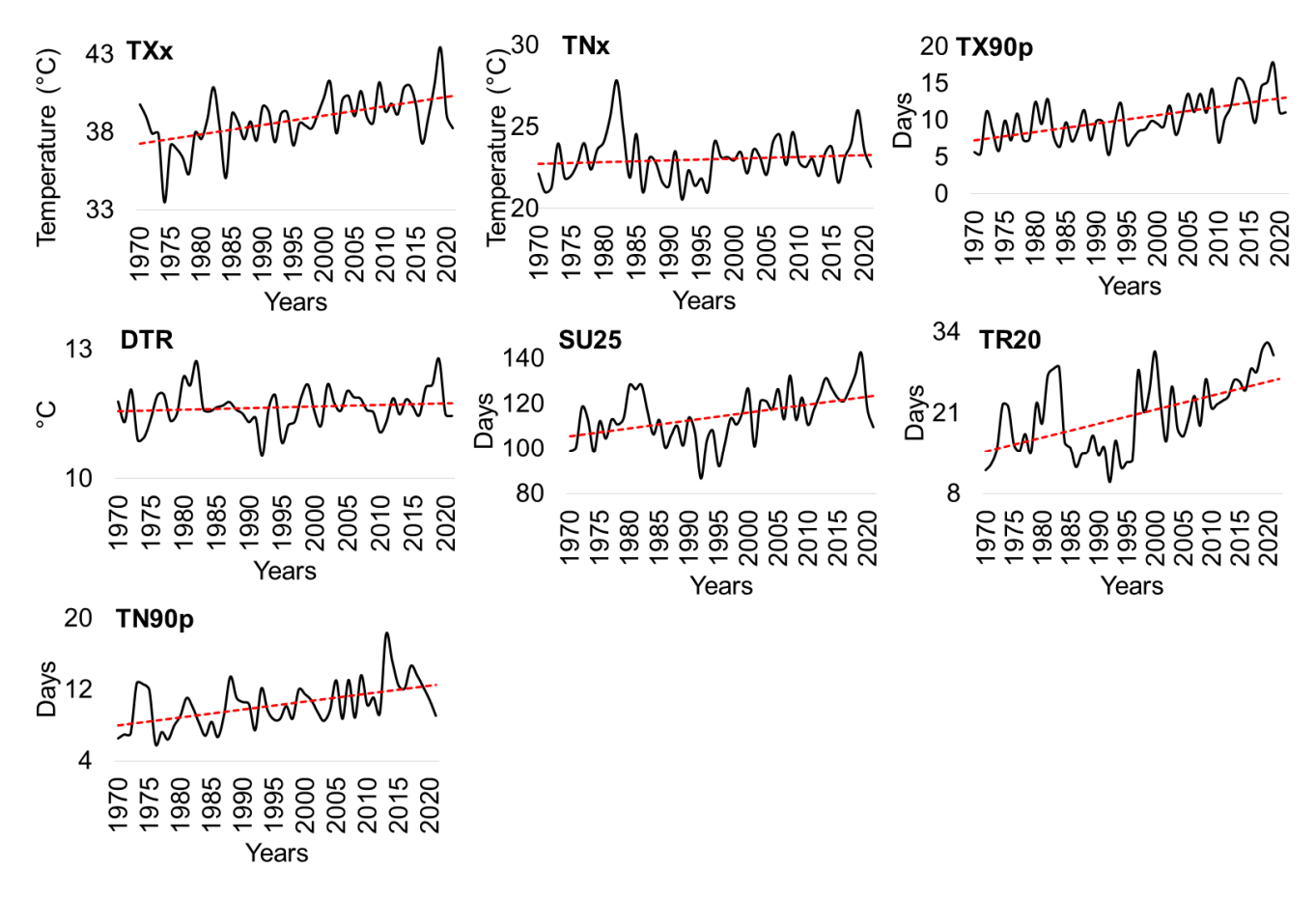


Figure 5. Regional behaviour of the extreme hot events. Results for hottest days (TXx), the maximum monthly value of the daily minimum temp (TNx), warm nights (TX90p), DTR, summer days (SU25), tropical nights (TR20), and warm days (TN90p) are shown. The red dot-dash line indicates the slope for the study period.

3.3. Extreme Cold Temperature Events

The spatial distribution of extreme cold events is presented in Figure 6. Coolest Days (TXn) shows an increase of up to 3 $^{\circ}$ C per period in the north, northeast, and west of SA. However, statistical significance was only identified in 35% of the area. The TNn shows a heterogeneous pattern, with values oscillating between -3 $^{\circ}$ C and 3.4 $^{\circ}$ C per period. Frost days (FD0) show a general decrease in most of the study area (68% of the weather stations). Consistent with extreme hot events, cold events also indicate global warming signals by increasing the minimum value of the maximum temperature and reducing frost days (Figure 6).

Water 2024, 16, 351 10 of 18

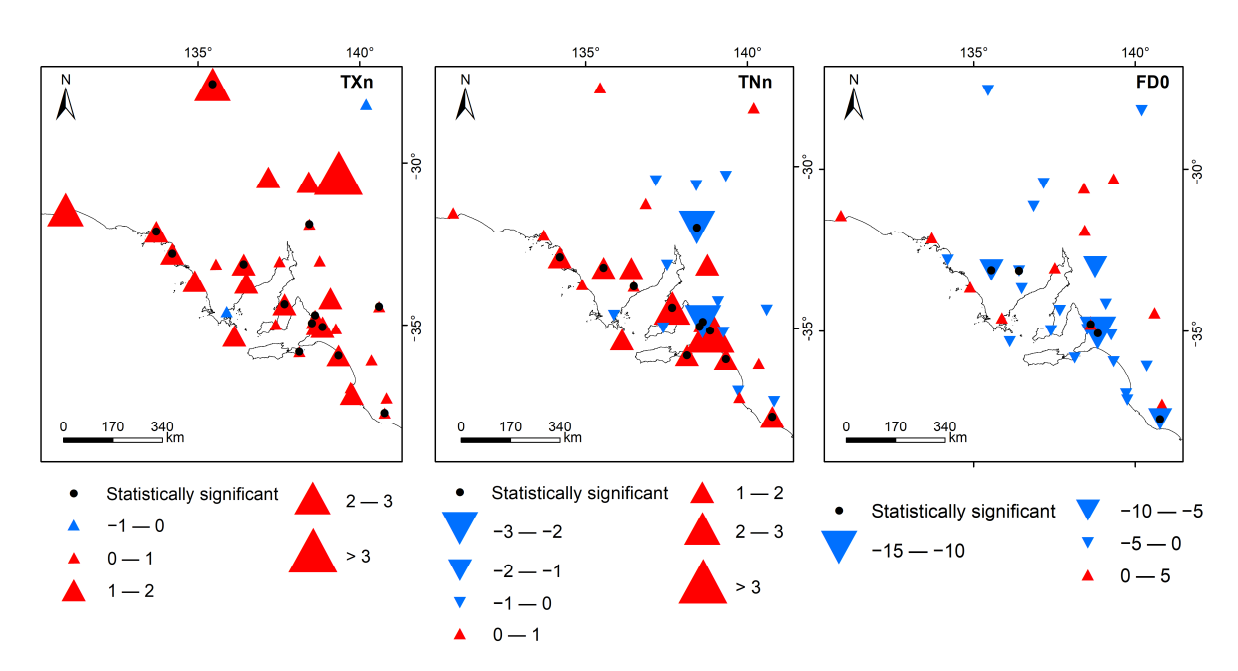


Figure 6. Trends and significance of Extreme cold events in SA. Results for the monthly minimum value of the daily maximum temperature (TXn), the monthly minimum value of the daily maximum temperature (TNn), and frost days (FDO) are shown. The triangles indicate positive trends (in red) and negative trends (in blue), along with their intensity. The black dots indicate the statistical significance of the slope.

At the regional scale, we observed an increase of $0.4~^{\circ}\text{C}$ per period in hottest days (TXx), but there was no significant evidence. The monthly minimum value of the daily maximum temp (TNn) registered a rise of $+0.9~^{\circ}\text{C}$ from 1970 to 2021. Finally, frost days (FD0) were significantly reduced by 6.2 days per period (Figure 7).

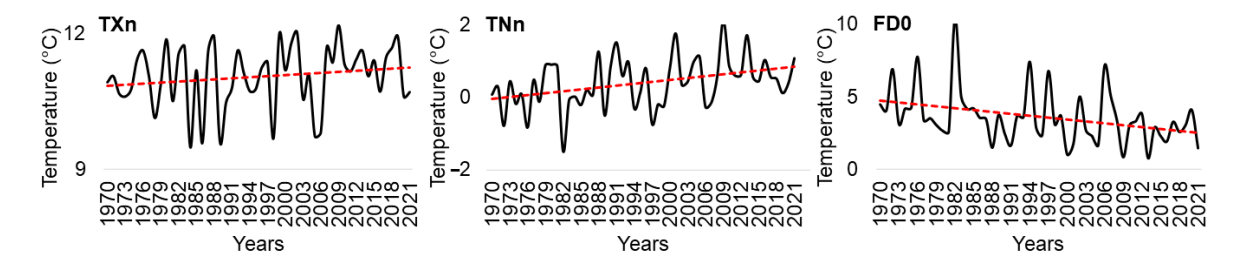


Figure 7. Regional behaviour of the Cold Extremes. Results for the monthly minimum value of the daily maximum temperature (TXn), the monthly minimum value of the daily maximum temperature (TNn), and frost days (FDO) are shown. The red dot-dash line indicates the slope for the study period.

3.4. Daily Rainfall Events

Rainfall events were subdivided into general events and those related to storms and wet days. Figure 8 presents the spatial distribution of Consecutive Dry Days (CDD), Consecutive Wet Days (CWD), SDII, Rx1day, and Rx5days. As observed during the precipitation trend analysis, most indices showed negative trends (CDD, CWD, and SDII). However, some areas were identified where the precipitation changed for one and five days. These areas, located in the central north of SA and the coast, registered an increase of up to 16 mm in Rx1day and 20 mm in Rx5days from 1970 to 2021. This situation is related to more severe rainfall events in the study area (Figure 8).

Water 2024, 16, 351 11 of 18

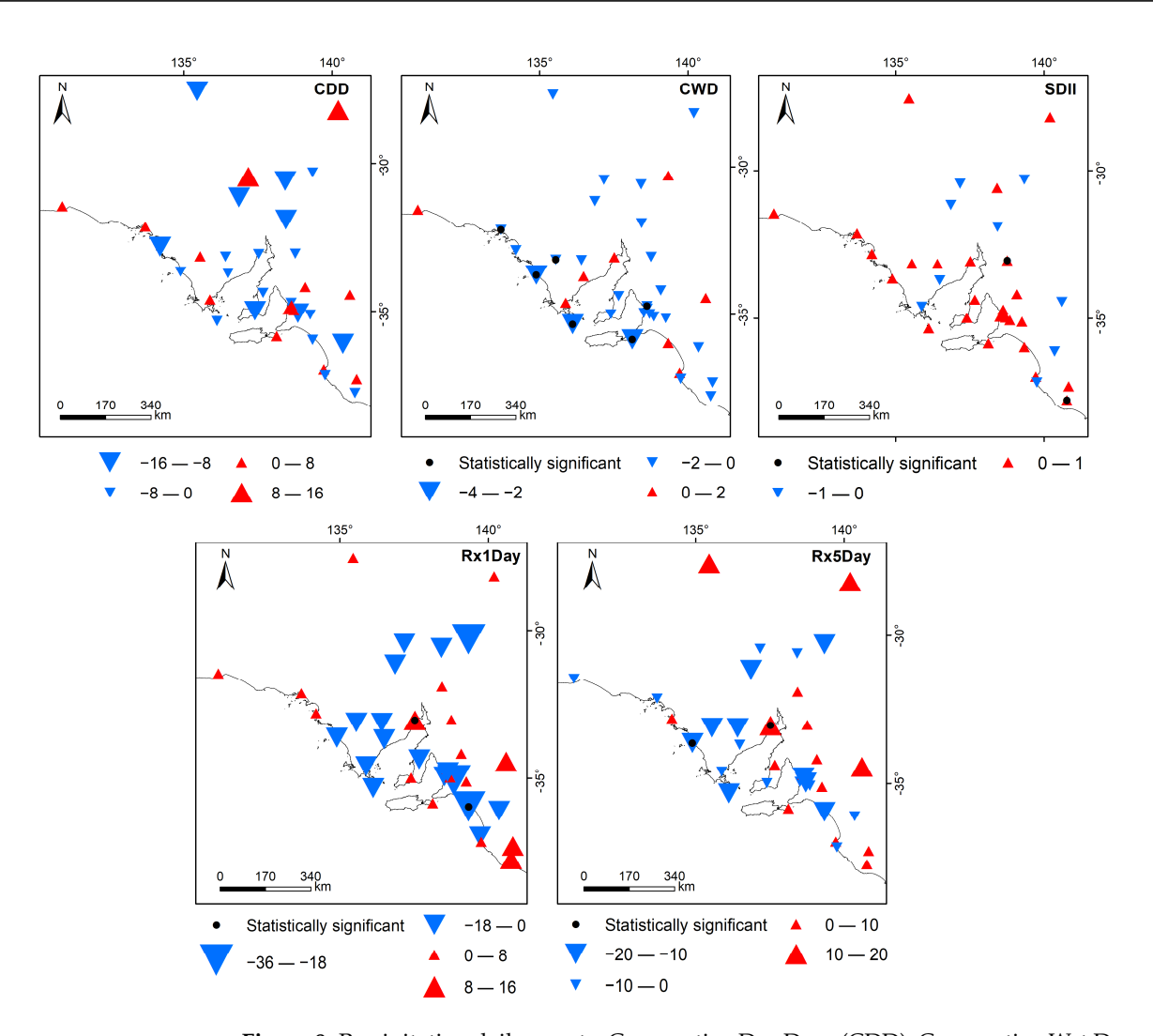


Figure 8. Precipitation daily events. Consecutive Dry Days (CDD), Consecutive Wet Days (CWD), annual total precipitation divided by the number of wet days in the year (SDII), Monthly maximum 1-day precipitation (Rx1day), and Monthly maximum consecutive 5-day precipitation (Rx5days) are shown. The triangles indicate positive trends (in red) and negative trends (in blue), along with their intensity. The black dots indicate the statistical significance of the slope.

SA did not represent statistical changes in these indices at a regional scale, except for CWD. The CDD showed oscillations related to the rainfall variability of the study area. The instability of consecutive wet days was -1.9 days per period (p < 0.05), but it was higher in coastal regions (-4.8 days per period). The same pattern was observed in the analyses of Rx1day and Rx5days (Figure 9).

Precipitation and wet days demonstrated a heterogeneous pattern. Heavy rainfall increased in coastal areas by more than 5 mm during 1970–2021 but decreased in the continental region. Extremely heavy storms (R20p) are generally reduced in the region, except for the coastal zone in the central north and central east. Very heavy precipitation (R30p) had a similar pattern to R20p, but they demonstrated increased extreme precipitation events. Despite this, the changes observed in the study period are not climatically significant (Figure 10). Wet days (R95p) showed critical changes. They reduced from 20 to 60 days per period in the north and by more than 20 days per period in the south and coastal areas. Very wet days (R99p) showed similar behaviour, but the increase was less (3.2 days per period; Figure 10). The trend analyses for the 50-year study period demonstrated that heavy precipitation increased by 0.3 mm. The rest of the indices showed a negative trend in the region but with slight variations (Figure 11).

Water **2024**, 16, 351

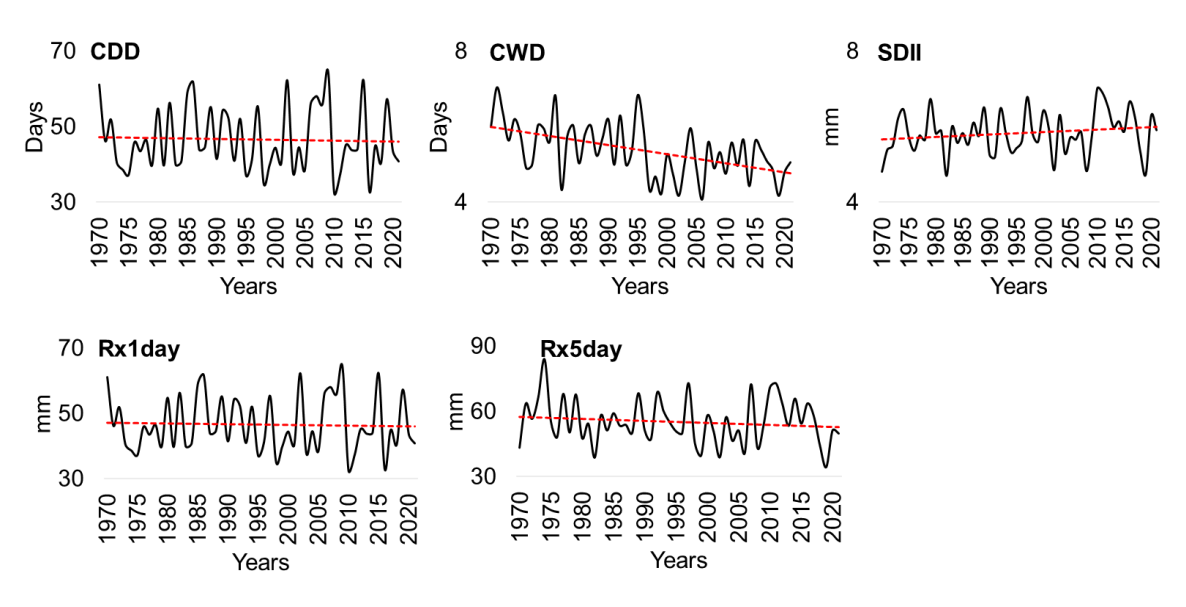


Figure 9. Regional behaviour of some precipitation indices. The red dot-dash line indicates the slope for the study period.

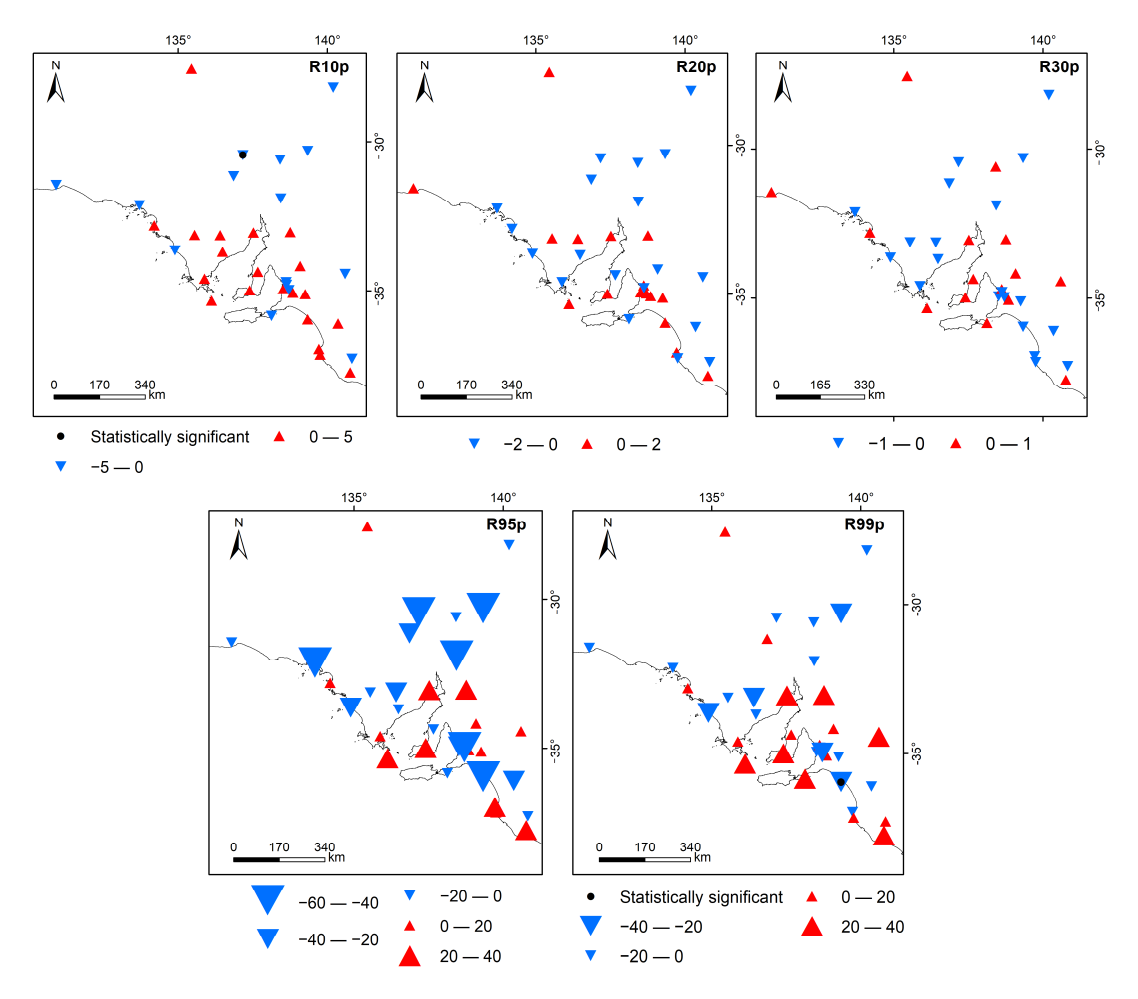


Figure 10. Precipitation daily events. R10p, R20p, and R30p indicate the annual count of days when the annual total wet-day precipitation PRCP > 10 mm, > 20 mm, or > 30 mm, respectively, and R95p and R99p indicate the annual total PRCP when RR > 95th and > 99th percentile respectively. The triangles indicate positive trends (in red) and negative trends (in blue), along with their intensity. The black dots indicate the statistical significance of the slope.

Water 2024, 16, 351 13 of 18

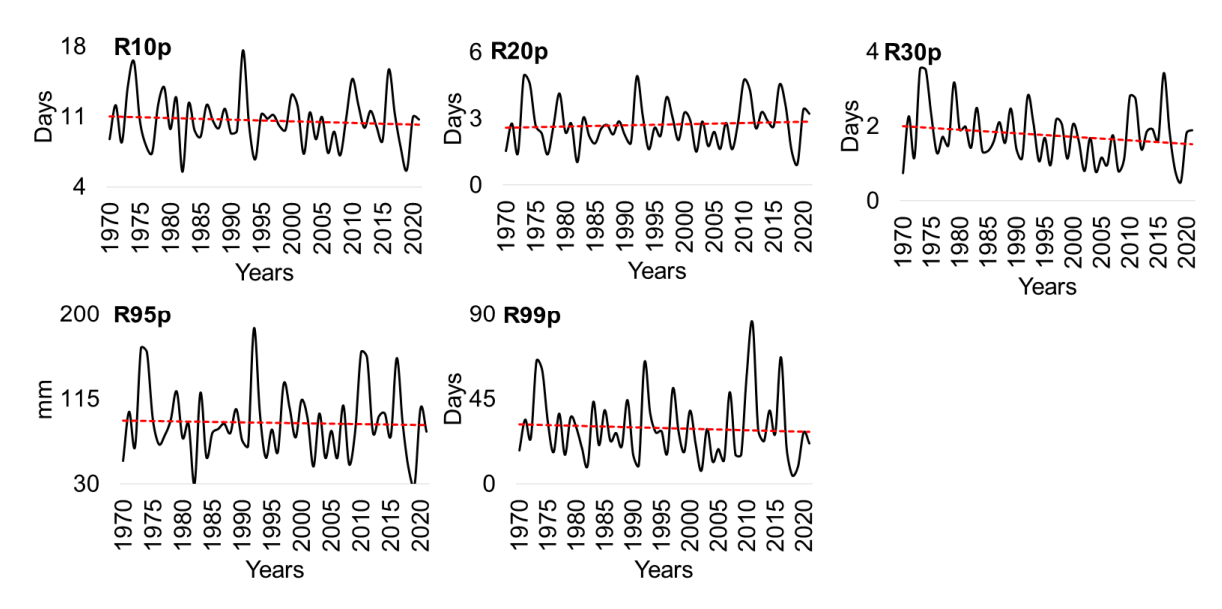


Figure 11. Regional behaviour of precipitation, wet, and very wet days. The red dot-dash line indicates the slope for the study period.

4. Discussion

The assessment of extreme temperature and rainfall events in South Australia showed signals of the effects of global warming. Analyses of trends at local and regional scales allow us to identify spatial and temporal changes over the last 50 years. The importance of applying this methodology is demonstrated by its ability to detect thermal and rainfall patterns worldwide [20,21,30]. Global warming triggers particular climate extremes, including increasing frequency of cold nights and days and growing warm days and nights [36]. The analysis of extreme hot events identified a generally positive trend, demonstrating the region's exposure to the effects of global warming, which is observed in other temperate areas of the Southern Hemisphere [21] and many other regions of the world [31,37,38].

In this context, it is crucial to emphasise that there are significant signs of global warming evidence in the Southern Hemisphere. For instance, the Pampas Region in Argentina has experienced substantial increases in maximum, minimum, and mean temperatures (1.8 $^{\circ}$ C, 1.2 $^{\circ}$ C, and 1.2 $^{\circ}$ C, respectively). These data reveal a notable consistency, suggesting that temperate climate regions in the Southern Hemisphere may be undergoing widespread warming, posing new challenges and the urgent need to implement adaptation and mitigation strategies in response to climate change [21,39,40].

Regarding precipitation, a projection of decreased rainfall has been observed in the Pampas Region in future climate change scenarios, with a clear trend toward aridity [41]. Moreover, daily rainfall events exhibit similarities to those observed in SA, showing heterogeneous variations, albeit with low statistical evidence. This indicates that while there may not be robust statistical evidence, changes in precipitation patterns are evident, with records of extreme and severe rainfall events, as well as an increase in consecutive dry days [37,41].

This demonstrates that there are localised regions in the Southern Hemisphere facing similar challenges as they will need to reconsider their plans for mitigating and adapting to global warming and the imminent impacts of climate change [42,43]. While Argentina and Australia are economically different countries, it is essential to recognise that these phenomena are impacting on a global scale. Therefore, it is imperative to develop sustainable land management policies to address these issues [6]. It is worth noting that the Pampas Region is one of the most fertile and important plains in the world, with the capacity to produce food for a significant portion of the planet. On the other hand, the state of South Australia has a significant regional and global interest due to its crops and extensive

Water 2024, 16, 351 14 of 18

livestock activities, among other factors. In this context, it is important to raise awareness about mitigation and adaptation plans [44].

Given the backdrop of global warming and climate change, it is important to acknowledge the necessity for specific policy recommendations that address the heightened risks and difficulties stemming from the continuously shifting environmental conditions [45]. Within this framework, it becomes imperative to consistently update land management plans and conduct thorough assessments that comprehensively evaluate the impacts of global warming associated with climate change. This entails examining historical and current climate data alongside projected alterations in temperature and precipitation patterns within the context of climate change. Such a context amplifies the susceptibility of ecosystems and communities to daily extreme events. Identifying and delineating high-risk and vulnerable areas is crucial for effectively prioritising resources and directing efforts accordingly [46].

Additionally, significant increases were observed in summer days and tropical nights in SA. Cold events registered similar patterns as extreme hot events, with an increase in minimum temperature that impacted the number of frost days. The reduction in the number of frost days and the increase in cold and hot events are related mainly to excessive heat, which may dry the soil and inhibit vegetation growth [20]. These changes could affect croplands and livestock in SA, two susceptible activities related to the change in thermal patterns. Furthermore, the positive and significant temperature trend demonstrated its effects on crop flowering, delaying the growing season and shortening the critical period, generating diminishing yields [47]. Remarkably, the effects on the growing season are a consequence of the increment of minimum temperature. However, in temperate climates, the increase in minimum temperature could create longer growing seasons during autumn and spring [40,48].

While the temperature increases homogeneously, precipitation has a heterogeneous pattern, as is common worldwide. Changes in thermal and rainfall patterns observed in South Australia evidence the effects of global warming. The most critical impact of these changes is related to the ecological environment due to reducing environmental services [49]. Along the same line, the hydrological cycle could be affected because of the increase in evapotranspiration and extreme rainfall events [50]. One of the most significant impacts of global warming is its effect on the population. South Australia has over 1.8 million inhabitants, and it is demonstrated that this phenomenon affects the quality of life. For instance, the increase in maximum temperature could severely impact cardiovascular and respiratory diseases [51], vector-borne diseases, and rise in mortality rates [50].

It is crucial to underscore that prior research has substantiated the presence of indicators signalling global warming and alterations in precipitation patterns within Australia. Specifically, in the southeastern region of the country, the existence of more intense and arid conditions during the 1911–2008 period has been firmly established. These alterations exert an influence on annual, seasonal, and daily extremes [52]. Moreover, in addition to the aforementioned findings, empirical evidence indicates that in the context of climate change scenarios associated with two Representative Concentration Pathways (RCP4.5 and RCP 8.5), cold temperature extremes are anticipated to experience a substantial reduction by the close of the 21st century, while warm temperature extremes are expected to escalate. Concurrently, while shifts in precipitation are projected to be less conspicuous, it has been observed that, towards the end of the century, there will be a heightened occurrence of dry periods. Simultaneously, the most intense precipitation extremes are predicted to intensify, contingent upon the specific emission scenarios considered [53].

Taking into account what will unfold in South Australia in the future under this scenario, it is essential to emphasise that the southwestern region of Australia will encounter elevated temperatures and corresponding increases in heat extremes attributed to greenhouse gas-induced forcing. In this context, the annual mean temperature is projected to rise by over 6 °C by the year 2100 under a high greenhouse gas emission scenario. Additionally,

Water 2024, 16, 351 15 of 18

a significant increase in drought occurrences is anticipated, associated with a decrease in precipitation during the southern hemisphere's winter season [53].

Extreme precipitation events may lead to an increase in the intensity and frequency of flooding, which can impose substantial costs on aquatic and terrestrial ecosystems, human societies, and the economy. Changes in flood characteristics not only depend on the spatial distribution, time evolution, and rarity of precipitation but also on antecedent soil moisture conditions [54,55]. In our study, we identified a decrease in the annual total wet-day precipitation across the entire area. However, despite the overall decrease in precipitation during the study period, extreme rainfall events increased in the central-eastern and coastal regions of South Australia. According to [52], precipitation extremes may change differently from total precipitation. The simplest expectation is that precipitation extremes should scale with low-level atmospheric moisture content, which increases at a rate of about 6–7% K⁻¹ warming, as predicted by the Clausius–Clapeyron relationship [52]. Therefore, global warming and anthropogenic aerosols are considered major components affecting extreme precipitation changes, e.g., [54,55].

The South Australia region has undergone significant changes in land use and coverage during the period 1990–2015. For instance, native vegetation increased by 0.5%, contrasting with a 0.9% decrease in non-native vegetation. Dryland agriculture experienced a 0.3% increase, whereas urban areas and built surfaces also expanded, albeit by 2.1% [56]. Indeed, it is anticipated that the rise in urbanisation will have a pronounced impact on minimum temperatures and, to a lesser extent, maximum temperatures in the near future [57].

Another crucial determinant of the temperature increase is the rise in greenhouse gas emissions (GHG). In Australia, agriculture ranks as the second-largest contributor to the country's GHG emissions, accounting for 14% [58], with livestock responsible for 70% of the total emissions. It is estimated that agricultural emissions will increase to 8–8.4% by 2020–2030, with an average of 8.3 Pg CO₂-eq by 2030 [59]. In this context, technological innovation and entrepreneurial activity can help address global warming by developing new technologies that reduce the cost of renewable energy or increase the efficiency of existing technologies; entrepreneurs can help drive the transition to a low-carbon economy [60].

The recent advancement of smart technologies has enabled the vision of smart farming (alternatively known as smart agriculture) based precision agriculture. The aim of smart farming is to improve productivity by increasing crop yields and profitability and reduce the environmental footprint, such as GHG emissions, by utilising different techniques such as efficient irrigation [61], targeted and precise use of pesticides and fertilisers for crops, etc. In addition, IoT enables the reduction of the inherent environmental impact by performing real-time detection of weeds or infestations [62] and monitoring weather conditions, soil conditions, etc., which consequently reduces and allows for adequate use of inputs such as water, pesticides, or agro-chemicals [61]. Livestock Farming: Smart livestock farming helps monitor animal grazing in open pastures or their location in big stables [63]. Smart farming also helps in detecting and maintaining air quality, ventilation in farms, and detecting and reducing GHG emissions from farms.

Finally, it is necessary to provide crucial information for stakeholders to design adaptation and mitigation strategies for reducing the effects of climate change. The relevance of the results obtained in this manuscript could be the basis for generating a management plan oriented to mitigate the adverse impacts on crop yield, grasslands, livestock, and water availability [20] and improve human life quality [21,63]. Trend analyses based on daily data demonstrate an essential tool for generating management plans focused on environmental sustainability [64].

5. Conclusions

We have identified the magnitude, intensity, and persistence of global warming signals over the last 50 years in South Australia using 24 climate extreme indices. We found remarkable warming signal trends in both hot and cold extreme events. Cold indices, such

Water 2024, 16, 351 16 of 18

as Frost days, showed negative trends, while the monthly minimum value of the daily maximum temperature (TXn) and the monthly minimum value of the daily minimum temperature (TNn) registered an increase. Moreover, most extreme hot events, such as summer days, warm days and nights, and tropical nights, presented a significant and positive change in most of the study area.

Rainfall had different impacts on local and regional scales. However, the analysis of precipitation presented a heterogeneous pattern. We demonstrated that although rain is decreasing regionally, heavy and extreme storms have become more severe locally in the last 50 years.

Finally, it is worth noting that based on the evidence presented in this manuscript, it would be crucial to generate or reorient sustainable management plans to mitigate and adapt to changes in the structure and function of ecosystems and reduce human diseases related to global warming.

Author Contributions: F.F.: Conceptualization, Data curation, Investigation, Methodology, Resources, Visualisation, Writing—original draft, Writing—review, editing, and funding. M.P.A.: Conceptualization, Data curation, Investigation, Visualisation, Resources, Writing—original draft, Writing—review and editing. A.S.B. and A.I.C.: Conceptualization, Data curation, Investigation, Visualisation, Resources, Writing—original draft, Writing—review and editing. P.A.H.: Conceptualisation, Funding acquisition, Investigation, Methodology, Project administration, Resources, Supervision, Visualisation, Writing—review and editing. All authors have read and agreed to the published version of the manuscript.

Funding: We duly acknowledge the National Council of Scientific and Technical Research and the FONCYT for funding this research through the projects PICT-2021-I-INVI-00580 and PIBAA 28720210100943CO. Furthermore, the authors would like to acknowledge Flinders University (SA, Australia).

Data Availability Statement: The data that supports this study will be shared, upon reasonable request, with the corresponding author. The information is available in the following links: http://www.bom.gov.au/https://etccdi.pacificclimate.org/list_27_indices.shtml (accessed on 30 December 2023).

Acknowledgments: We would like to thank the Bureau of Meteorology of Australia for providing meteorological data.

Conflicts of Interest: The authors declare that they have no conflicts of interest.

References

- 1. Roubille, F.; Matzner-Lober, E.; Aguilhon, S.; Rene, M.; Lecourt, L.; Galinier, M.; Molinari, N. Impact of global warming on weight in patients with heart failure during the 2019 heatwave in France. ESC Heart Fail. 2023, 10, 727–731. [CrossRef] [PubMed]
- 2. Zhuang, X.; Hao, Z.; Singh, V.P.; Zhang, Y.; Feng, S.; Xu, Y.; Hao, F. Drought propagation under global warming: Characteristics, approaches, processes, and controlling factors. *Sci. Total Environ.* **2022**, *838*, 156021. [CrossRef] [PubMed]
- 3. Woolway, R.I.; Albergel, C.; Frölicher, T.L.; Perroud, M. Severe Lake Heatwaves Attributable to Human-Induced Global Warming. *Geophys. Res. Lett.* **2022**, 49, e2021GL097031. [CrossRef]
- 4. Evans, G.W. Projected behavioral impacts of global climate change. Annu. Rev. Psychol. 2019, 70, 449–474. [CrossRef]
- 5. Li, Z.; Fang, G.; Chen, Y.; Duan, W.; Mukanov, Y. Agricultural water demands in Central Asia under 1.5 °C and 2.0 °C global warming. *Agric. Water Manag.* **2020**, 231, 106020. [CrossRef]
- 6. Diffenbaugh, N.S.; Burke, M. Global warming has increased global economic inequality. *Proc. Natl. Acad. Sci. USA* **2019**, *116*, 9808–9813. [CrossRef]
- 7. Ocko, I.B.; Sun, T.; Shindell, D.; Oppenheimer, M.; Hristov, A.N.; Pacala, S.W.; Hamburg, S.P. Acting rapidly to deploy readily available methane mitigation measures by sector can immediately slow global warming. *Environ. Res. Lett.* **2021**, *16*, 054042. [CrossRef]
- 8. Stark, C.; Thompson, M.; Andrew, T.; Beasley, G.; Bellamy, O.; Budden, P.; Vause, E. Net Zero: The UK's Contribution to Stopping Global Warming; Climate Change Committee: London, UK, 2019.
- 9. Parker, T.; Gallant, A.; Hobbins, M.; Hoffmann, D. Flash drought in Australia and its relationship to evaporative demand. *Environ. Res. Lett.* **2021**, *16*, 064033. [CrossRef]
- 10. Phillips, N.; Nogrady, B. The race to decipher how climate change influenced Australia's record fires. *Nature* **2020**, 577, 610–613. [CrossRef]

Water **2024**, 16, 351 17 of 18

11. Xu, X.; Jia, G.; Zhang, X.; Riley, W.J.; Xue, Y. Climate regime shift and forest loss amplify fire in Amazonian forests. *Glob. Chang. Biol.* **2020**, *26*, 5874–5885. [CrossRef]

- 12. Abram, N.J.; Henley, B.J.; Sen Gupta, A.; Lippmann, T.J.; Clarke, H.; Dowdy, A.J.; Boer, M.M. Connections of climate change and variability to large and extreme forest fires in southeast Australia. *Commun. Earth Environ.* **2021**, *2*, 8. [CrossRef]
- 13. McGowan, H.; Theobald, A. Atypical weather patterns cause coral bleaching on the Great Barrier Reef, Australia during the 2021–2022 La Niña. *Sci. Rep.* **2023**, *13*, 6397. [CrossRef] [PubMed]
- 14. Schneider, M.; Radbone, C.G.; Vasquez, S.A.; Palfy, M.; Stanley, A.K. Population data centre profile: SA NT DataLink (South Australia and Northern Territory). *Int. J. Popul. Data Sci.* **2019**, *4*, 1136. [CrossRef] [PubMed]
- 15. Rose, T.J.; Parvin, S.; Han, E.; Condon, J.; Flohr, B.M.; Schefe, C.; Kirkegaard, J.A. Prospects for summer cover crops in southern Australian semi-arid cropping systems. *Agric. Syst.* **2022**, *200*, 103415. [CrossRef]
- 16. Ratnayake, D.C.; Hewa, G.A.; Kemp, D.J. Challenges in quantifying losses in a partly urbanised catchment: A south Australian case study. *Water* **2022**, *14*, 1313. [CrossRef]
- 17. Wang, B.; Gray, J.M.; Waters, C.M.; Anwar, M.R.; Orgill, S.E.; Cowie, A.L.; Li Liu, D. Modelling and mapping soil organic carbon stocks under future climate change in south-eastern Australia. *Geoderma* **2022**, 405, 115442. [CrossRef]
- 18. McGreevy, M.; MacDougall, C.; Fisher, M.; Henley, M.; Baum, F. Expediting a renewable energy transition in a privatised market via public policy: The case of south Australia 2004-18. *Energy Policy* **2021**, *148*, 111940. [CrossRef]
- 19. Simshauser, P.; Gilmore, J. Climate change policy discontinuity & Australia's 2016–2021 renewable investment supercycle. *Energy Policy* **2022**, *160*, 112648.
- 20. Worku, G.; Teferi, E.; Bantider, A.; Dile, Y.T. Observed changes in extremes of daily rainfall and temperature in Jemma sub-basin Upper Blue Nile Basin, Ethiopia. *Theor. Appl. Climatol.* **2019**, *135*, 839–854. [CrossRef]
- 21. Ferrelli, F.; Brendel, A.S.; Perillo, G.M.E.; Piccolo, M.C. Warming signals emerging from the analysis of daily changes in extreme temperature events over Pampas (Argentina). *Environ. Earth Sci.* **2021**, *80*, 422. [CrossRef]
- 22. Zhou, H.; Aizen, E.; Aizen, V. Constructing a long-term monthly climate data set in central Asia. *Int. J. Climatol.* **2018**, *38*, 1463–1475. [CrossRef]
- 23. Zhang, X.; Yang, F. RClimDex (1.1) User Manual. 2013. Available online: http://cccma.Seos.Uvic.Ca/ETCCDI/software.shtml (accessed on 25 October 2022).
- 24. Wang, X.L.; Wen, Q.H.; Wu, Y. Penalized maximal *t* test for detecting undocumented mean change in climate data series. *J. Appl. Meteorol. Climatol.* **2007**, *46*, 916–931. [CrossRef]
- 25. Wang, X.L. Penalized maximal F-test for detecting undocumented mean shifts without trend-change. *J. Atmos. Ocean. Technol.* **2008**, 25, 368–384. [CrossRef]
- 26. Ruml, M.; Gregorić, E.; Vujadinović, M.; Radovanović, S.; Matović, G.; Vuković, A.; Pocuca, V.; Stojičić, D. Observed changes of temperature extremes in Serbia over the period 1961–2010. *Atmos. Res.* **2017**, *183*, 26–41. [CrossRef]
- 27. Taylor, M.H.; Losch, M.; Wenzel, M.; Schröter, J. On the sensitivity of eld reconstruction and prediction using empirical orthogonal functions derived from Gappy data. *J. Clim.* **2013**, *26*, 9194–9205. [CrossRef]
- 28. Kondrashov, D.; Denton, R.; Shprits, Y.Y.; Singer, H.J. Reconstruction of gaps in the past history of solar wind parameters. *Geophys. Res. Lett.* **2014**, *41*, 2702–2707. [CrossRef]
- 29. Zhang, Q.; Li, J.; Chen, Y.D.; Chen, X. Observed changes of temperature extremes during 1960–2005 in China: Natural or human-induced variations? *Theor. Appl. Climatol.* **2011**, *106*, 417–431. [CrossRef]
- 30. Ferrelli, F.; Brendel, A.S.; Aliaga, V.S.; Piccolo, M.C.; Perillo, G.M.E. Climate regionalization and trends based on daily temperature and precipitation extremes in the south of the Pampas (Argentina). *Cuad. Investig. Geogr.* **2019**, *45*, 393–416. [CrossRef]
- 31. Chen, A.; He, X.; Guan, H.; Cai, Y. Trends and periodicity of daily temperature and precipitation extremes during 1960–2013 in Hunan Province, central south China. *Theor. Appl. Climatol.* **2017**, 132, 71–88. [CrossRef]
- 32. Mann, H.B. Non-parametric tests against trend. Econométrica 1945, 13, 245–259. [CrossRef]
- 33. Kendall, M.R. Rank Correlation Methods, 4th ed. Chareles Griffin: London, UK, 1955.
- 34. Pohlert, T. Non-parametric trend tests and change-point detection. CC BY-ND 2016, 4, 1–18.
- 35. Hamed, K.H. Trend detection in hydrologic data: The Mann–Kendall trend test under the scaling hypothesis. *J. Hydrol.* **2008**, 349, 350–363. [CrossRef]
- 36. Alhaji, U.U.; Yusuf, A.S.; Edet, C.O.; Oche, C.O.; Agbo, E.P. Trend analysis of temperature in Gombe state using mann kendall trend test. *J. Sci. Res. Rep.* **2018**, *20*, 1–9. [CrossRef]
- 37. Peterson, T.; Folland, C.; Gruza, G.; Hogg, W.; Mokssit, A.; Plummer, N. Report on the Activities of the Working Group on Climate Change Detection and Related Rapporteurs; World Meteorological Organization: Geneva, Switzerland, 2001; p. 146.
- 38. Sun, W.; Mu, X.; Song, X.; Wu, D.; Cheng, A.; Qiu, B. Changes in extreme temperature and precipitation events in the Loess Plateau (China) during 1960–2013 under global warming. *Atmos. Res. Lett.* **2016**, *168*, 33–48. [CrossRef]
- 39. Ferrelli, F. Remote Sensing applications for effective fire disaster management plans: A review. *Inf. Syst. Smart City* **2023**, *3*, 1–17. [CrossRef]
- 40. Ferrelli, F.; Brendel, A.S.; Piccolo, M.C.; Perillo, G.M.E. Tendencia actual y futura de la precipitación en el sur de la Región Pampeana (Argentina). *Investig. Geogr.* **2020**, *102*. [CrossRef]
- 41. Ferrelli, F.; Brendel, A.; Piccolo, M.C.; Perillo, G.M.E. Evaluación de la tendencia de la precipitación en la región pampeana (Argentina) durante el período 1960–2018. *RA'EGA* **2021**, *51*, 41–57. [CrossRef]

Water **2024**, 16, 351 18 of 18

42. Gérard, M.; Vanderplanck, M.; Wood, T.; Michez, D. Global warming and plant–pollinator mismatches. *Emerg. Top. Life Sci.* **2020**, 4,77–86.

- 43. Deng, K.; Azorin-Molina, C.; Yang, S.; Hu, C.; Zhang, G.; Minola, L.; Chen, D. Changes of Southern Hemisphere westerlies in the future warming climate. *Atmos. Res.* **2022**, *270*, 106040. [CrossRef]
- 44. Abbass, K.; Qasim, M.Z.; Song, H.; Murshed, M.; Mahmood, H.; Younis, I. A review of the global climate change impacts, adaptation, and sustainable mitigation measures. *Environ. Sci. Pollut. Res.* **2022**, *29*, 42539–42559. [CrossRef]
- 45. Zandalinas, S.I.; Fritschi, F.B.; Mittler, R. Global warming, climate change, and environmental pollution: Recipe for a multifactorial stress combination disaster. *Trends Plant Sci.* **2021**, *26*, 588–599. [CrossRef] [PubMed]
- 46. Fernández-Long, M.E.; Müller, G.V.; Beltrán-Przekurat, A.; Scarpati, O.E. Long-term and recent changes in temperature-based agroclimatic indices in Argentina. *Int. J. Climatol.* **2013**, *33*, 1673–1686. [CrossRef]
- 47. Sun, W.; Song, X.; Mu, X.; Gao, P.; Wang, F.; Zhao, G. Spatiotemporal vegetation cover variations associated with climate change and ecological restoration in the Loess Plateau. *Agric. Meteorol.* **2015**, 209, 87–99. [CrossRef]
- 48. Zilio, M.I.; Alfonso, M.B.; Ferrelli, F.; Perillo, G.M.E.; Piccolo, M.C. Ecosystem services provision, tourism and climate variability in shallow lakes: The case of La Salada, Buenos Aires, Argentina. *Tour. Manag.* **2017**, *62*, 208–217. [CrossRef]
- 49. Thakuri, S.; Dahal, S.; Shrestha, D.; Guyennon, N.; Romano, E.; Colombo, N.; Salerno, F. Elevation-dependent warming of maximum air temperature in Nepal during 1976–2015. *Atmos. Res. Lett.* **2019**, 228, 261–269. [CrossRef]
- 50. Lim, S.S.; Vos, T.; Flaxman, A.D.; Danaei, G.; Shibuya, K.; Adair-Rohani, H.; Aryee, M. A comparative risk assessment of burden of disease and injury attributable to 67 risk factors and risk factor clusters in 21 regions, 1990–2010: A systematic analysis for the Global Burden of Disease Study 2010. *Lancet* 2012, 380, 2224–2260. [CrossRef] [PubMed]
- 51. Gallant, A.J.; Karoly, D.J. A combined climate extremes index for the Australian region. J. Clim. 2010, 23, 6153–6165. [CrossRef]
- 52. Alexander, L.V.; Arblaster, J.M. Historical and projected trends in temperature and precipitation extremes in Australia in observations and CMIP5. *Weather. Clim. Extrem.* **2017**, *15*, 34–56. [CrossRef]
- 53. Grose, M.R.; Narsey, S.; Delage, F.P.; Dowdy, A.J.; Bador, M.; Boschat, G.; Power, S. Insights from CMIP6 for Australia's future climate. *Earth's Future* **2020**, *8*, e2019EF001469. [CrossRef]
- 54. Sharma, A.; Wasko, C.; Lettenmaier, D.P. If precipitation extremes are increasing, why aren't foods? *Water Resour. Res.* **2018**, *54*, 8545–8551. [CrossRef]
- 55. Blöschl, G.; Hall, J.; Parajka, J.; Perdigão, R.A.; Merz, B.; Arheimer, B.; Živković, N. Changing climate shifts timing of European floods. *Science* **2017**, *357*, 588–590. [CrossRef] [PubMed]
- 56. Willoughby, N.; Thompson, D.; Royal, M.; Miles, M. South Australian Land Cover Layers: An Introduction and Summary Statistics; Department for Environment and Water: Adelaide, Australia, 2018.
- 57. Climate Council of Australia. Australia's Rising Greenhouse Gas Emissions; Climate Council: Potts Point, Australia, 2018.
- 58. Panchasara, H.; Samrat, N.H.; Islam, N. Greenhouse gas emissions trends and mitigation measures in Australian agriculture sector—A review. *Agriculture* **2021**, *11*, 85. [CrossRef]
- 59. Trenberth, K.E. Understanding climate change through Earth's energy flows. J. R. Soc. N. Z. 2020, 50, 331–347. [CrossRef]
- 60. Islam, N.; Ray, B.; Pasandideh, F. IoT based smart farming: Are the LPWAN technologies suitable for remote communication? In Proceedings of the 2020 IEEE International Conference on Smart Internet of Things (SmartIoT), Beijing, China, 14–16 August 2020; pp. 270–276.
- 61. Alam, M.; Alam, M.S.; Roman, M.; Tufail, M.; Khan, M.U.; Khan, M.T. Real-time machine-learning based crop/weed detection and classification for variable-rate spraying in precision agriculture. In Proceedings of the 2020 7th International Conference on Electrical and Electronics Engineering (ICEEE), Antalya, Turkey, 14–16 April 2020; pp. 273–280.
- Saravanan, K.; Saraniya, S. Cloud IOT based novel livestock monitoring and identification system using UID. Sens. Rev. 2017, 38, 21–33.
- 63. Xu, M.J.; Plonowska, K.A.; Gurman, Z.R.; Humphrey, A.K.; Ha, P.K.; Wang, S.J.; El-Sayed, I.H.; Heaton, C.M.; George, J.R.; Yom, S.S.; et al. Treatment modality impact on quality of life for human papillomavirus—associated oropharynx cancer. *Laryngoscope* **2020**, *130*, E48–E56. [CrossRef]
- 64. Tierney, J.; Smerdon, J.; Anchukaitis, K.; Seager, R. Multidecadal variability in East African hydroclimate controlled by the Indian Ocean. *Nature* 2013, 493, 389–392. [CrossRef]

Disclaimer/Publisher's Note: The statements, opinions and data contained in all publications are solely those of the individual author(s) and contributor(s) and not of MDPI and/or the editor(s). MDPI and/or the editor(s) disclaim responsibility for any injury to people or property resulting from any ideas, methods, instructions or products referred to in the content.